Chinese Journal of Aeronautics, (2023), **xxx**(xx): xxx–xxx

Chinese Society of Aeronautics and Astronautics
& Beihang University

Chinese Journal of Aeronautics

cja@buaa.edu.cn
www.sciencedirect.com

FULL LENGTH ARTICLE

Attitude control of multi-spacecraft systems on SO (3) with stochastic links failure

KANG Zeyu [a], SHEN Qiang [a], WU Shufan [a,*], Chris J. DAMAREN [b], MU Zhongcheng [a]

[a] *School of Aeronautics and Astronautics, Shanghai Jiao Tong University, Shanghai 200240, China*
[b] *Institute for Aerospace Studies, University of Toronto, Toronto, Ontario M3H 5T6, Canada*

Received 21 March 2023; revised 12 December 2023; accepted 12 December 2023

KEYWORDS

Multi-spacecraft systems;
Attitude consensus;
Attitude stabilization;
Stochastic links failure;
Super-martingale convergence

Abstract In this paper, for Multi-Spacecraft System (MSS) with a directed communication topology link and a static virtual leader, a controller is proposed to realize attitude consensus and attitude stabilization with stochastic links failure and actuator saturation. First, an MSS attitude error model suitable for a directed topology link and with a static virtual leader based on SO(3) is derived, which considers that the attitude error on SO(3) cannot be defined based on algebraic subtraction. Then, we design a controller to realize the MSS on SO(3) with attitude consensus and attitude stabilization under stochastic links failure and actuator saturation. Finally, the simulation results of a multi-spacecraft system with stochastic links failure and a static virtual leader spacecraft are demonstrated to illustrate the efficiency of the attitude controller.

© 2023 Production and hosting by Elsevier Ltd. on behalf of Chinese Society of Aeronautics and Astronautics. This is an open access article under the CC BY-NC-ND license (http://creativecommons.org/licenses/by-nc-nd/4.0/).

Uncorrected Proof

1. Introduction

In recent years, the attitude control of Multi-Spacecraft System (MSS) has aroused widespread concern. By using the information-based sharing, interaction and cooperation of the MSS to form a large virtual spacecraft, it can not only replace the role of large spacecraft in many application fields, but also obtain many advantages.[1] For example, in the process of carrying out deep space exploration and earth observation missions, the MSS can significantly improve the information processing and observation capability. In addition, the failure of one spacecraft in an MSS will not cause the failure of the whole mission, which improves the reliability and stability. Meanwhile, it has the advantages of cheap and easy maintenance.[2–5] Therefore, as a necessary extension and supplement to the technology of large spacecraft, the MSS technology has a very important research value.

At present, many attitude representation methods have been developed for rigid body attitude control.[6] These include Euler angles and Modified Rodriguez Parameters (MRPs), which have the disadvantage of singularities.[7] Thus, they are not suitable for large-angle attitude redirection maneuvers. The unit-quaternion in non-Euclidean global parameterization has no singularity. However, there is an unexpected ambiguity

* Corresponding author.
E-mail address: shufan.wu@sjtu.edu.cn (S. WU).
☆ Peer review under responsibility of Editorial Committee of CJA.

Production and hosting by Elsevier

https://doi.org/10.1016/j.cja.2023.12.019
1000-9361 © 2023 Production and hosting by Elsevier Ltd. on behalf of Chinese Society of Aeronautics and Astronautics.
This is an open access article under the CC BY-NC-ND license (http://creativecommons.org/licenses/by-nc-nd/4.0/).

phenomenon,[8] i.e., each rotation can be expressed by two different unit-quaternions. Accordingly, the attitude representation method of rigid spacecraft based on the Lie group SO(3) can avoid the defects of the above three attitude representations and has caused in-depth research. Four types of tracking control systems for a rigid spacecraft directly on the special orthogonal group SO(3) were designed by Lee[9] to achieve global exponential stability and to avoid singularities of local coordinates, or ambiguities associated with quaternions. An adaptive controller on SO(3) for a rigid spacecraft was derived by Kulumani et al.,[10] which can satisfy the attitude constraint and avoid the attitude-forbidden zone in the course of redirection.

In addition, for the attitude tracking problem of the MSS, all spacecraft have to track the desired attitude given by the virtual leader spacecraft. In order to reduce the communication burden and improve the robustness of the MSS, a distributed strategy has been widely used in missions,[11–15] i.e., each spacecraft can only determine its own control commands according to its own state and the communication with neighboring spacecraft. For the multi-spacecraft system on MRPs with both rigid and flexible spacecraft, a controller was designed by Du et al.[16] for each spacecraft to track the attitude of the virtual leader spacecraft. Cui et al.[17] proposed a distributed finite time attitude tracking controller with unavailable angular velocity on MRPs for uncertain MSS under directed topology conditions. An adaptive nonsingular fast terminal sliding mode controller was developed by Zhang et al.[18] for MSS using the unit-quaternion under directed and undirected graph to achieve attitude synchronization and tracking. For the multi-spacecraft system on unit-quaternion, in which only some spacecraft can obtain virtual leader commands, an adaptive attitude controller was designed by Yue et al.[19] to achieve attitude coordination and tracking under uncertain inertia parameters. An adaptive fault-tolerant controller on unit-quaternion was designed by Hu et al.[20] to realize the attitude coordination and tracking of multi-spacecraft system with the uncertain inertia parameters, the actuators failure, and the time-varying center of mass. Under a directed graph, a distributed adaptive controller was employed by Chen and Shan[21] for MSS on SO(3) to achieve attitude tracking and synchronization. Considering mixed attitude constraints, an saturated adaptive controller on SO(3) was designed by Kang et al.[22] to achieve attitude coordination and tracking of multiple spacecraft systems with arbitrary initial attitude. The above literature assumes that the communication links between spacecraft are determined, i.e., the links between spacecraft are 100% communicable, and stochastic links failure is not taken into account.

In practice, communication links between spacecraft are susceptible to multiple uncertainties, such as environmental disturbances, stochastic characteristics of equipment, and randomly lost package of data. Therefore, it is uncertain whether the communication link between spacecraft is connected, i.e., the link is possible to fail and be randomly reconstructed. A discrete-time protocol for discrete-time linear multi-agent systems was addressed by Rezaee et al.,[23] which achieved almost sure consensus under stochastic links failure. The attitude consensus problem in MSS using the unit-quaternion under stochastic link failures was studied by Rezaee and Abdollahi.[24] However, the model of the spacecraft is represented by the unit-quaternion, and it can not track the expected attitude due to only considering the attitude consensus, which limits the application in the mission. To the best of our knowledge, designing an attitude controller for MSS on SO(3) with a virtual leader spacecraft under stochastic links failure is still an open problem.

In this work, we consider that the MSS are connected in a directed topology, and a virtual leader spacecraft provides a static desired attitude for the MSS. It is assumed that each communication link between two spacecraft including the leader is not deterministic and may experience connection failure and be reconstructed randomly over time. To solve this challenging problem, a MSS attitude error model based on SO(3) suitable for a directed topology link is derived. Then, a controller is designed to realize the MSS on SO(3) with attitude consensus and attitude stabilization under stochastic links failure and actuator saturation.

The main contribution of this work is stated as follows:

Compared with the existing attitude control approaches[16,18,21,24] of MSS, we design an attitude controller for the MSS on SO(3) with a static virtual leader to realize attitude consensus and attitude stabilization under stochastic links failure and actuator saturation.

The remainder of this paper is organized as follows. The attitude kinematics and dynamics of MSS on SO(3) are modeled in Section 2. One problem to be solved in this paper is stated in Section 3. In Section 4, an MSS attitude stabilization error model on SO(3) suitable for a directed topology link and with a static virtual leader is proposed. The controller under the stochastic links failure is designed to realize the MSS attitude consensus and attitude stabilization on SO(3) in Section 5. Simulation results are demonstrated in Section 6. Conclusions are drawn in Section 7.

2. Preliminaries

2.1. Attitude kinematics and dynamics with actuator saturation

In this paper, the attitude dynamics of a rigid body is considered. Let $\mathscr{I}$ denote an inertial reference frame and $\mathscr{B}$ denote the body-fixed frame with origin being located at the center of mass. A special group of 3×3 orthogonal matrices used to parameterize attitude is defined as

$$\mathrm{SO}(3)=\left\{\boldsymbol{R}\in\mathbb{R}^{3\times 3}\,|\,\boldsymbol{R}^{\mathrm{T}}\boldsymbol{R}=\boldsymbol{I}_3,\det\boldsymbol{R}=1\right\}\tag{1}$$

The hat map $\wedge:\mathbb{R}^3\rightarrow\mathfrak{so}(3)$ is used to convert a vector in $\mathbb{R}^3$ to a 3×3 skew-symmetric matrix, where $\mathfrak{so}(3)$ is also the Lie algebra corresponding to the vector. More explicitly, for a vector $\boldsymbol{x}=[x_1,x_2,x_3]^{\mathrm{T}}\in\mathbb{R}^3$, we have

$$\hat{\boldsymbol{x}}=\begin{bmatrix}0 & -x_3 & x_2\\ x_3 & 0 & -x_1\\ -x_2 & x_1 & 0\end{bmatrix}\tag{2}$$

The inverse of the hat map is denoted by the vee map $\vee:\mathfrak{so}(3)\rightarrow\mathbb{R}^3$. Several properties of the hat map and the vee map of $\boldsymbol{x},\boldsymbol{y}\in\mathbb{R}^3$ are summarized as follows:[25,10]

$$\hat{\boldsymbol{x}}\boldsymbol{y}=\boldsymbol{x}\times\boldsymbol{y}=-\boldsymbol{y}\times\boldsymbol{x}=-\hat{\boldsymbol{y}}\boldsymbol{x}\tag{3}$$

$$\mathrm{tr}[\boldsymbol{A}\hat{\boldsymbol{x}}]=0.5\mathrm{tr}\left[\hat{\boldsymbol{x}}\left(\boldsymbol{A}-\boldsymbol{A}^{\mathrm{T}}\right)\right]=-\boldsymbol{x}^{\mathrm{T}}\left(\boldsymbol{A}-\boldsymbol{A}^{\mathrm{T}}\right)^{\vee}\tag{4}$$

Uncorrected Proof

$$\hat{\boldsymbol{x}}\boldsymbol{A} + \boldsymbol{A}^{\mathrm{T}}\hat{\boldsymbol{x}} = (\{\mathrm{tr}[\boldsymbol{A}]\boldsymbol{I}_3 - \boldsymbol{A}\}\boldsymbol{x})^{\wedge} \tag{5}$$

$$\boldsymbol{R}\hat{\boldsymbol{x}}\boldsymbol{R}^{\mathrm{T}} = (\boldsymbol{R}\boldsymbol{x})^{\wedge} \tag{6}$$

for any $\boldsymbol{x}, \boldsymbol{y} \in \mathbb{R}^3$, $\boldsymbol{A} \in \mathbb{R}^{3\times3}$ and $\boldsymbol{R} \in \mathrm{SO}(3)$.

Then, consider an MSS consisting of N spacecraft. Let $\boldsymbol{R}_i \in \mathrm{SO}(3)$ represent the rotation matrix of the i-th spacecraft from the body frame $\mathscr{B}$ to the inertial reference frame $\mathscr{I}$. The attitude kinematics of the i-th spacecraft can be expressed as[26,21]

$$\dot{\boldsymbol{R}}_i = \boldsymbol{R}_i\hat{\boldsymbol{\Omega}}_i \tag{7}$$

where $\boldsymbol{\Omega}_i \in \mathbb{R}^3$ is the inertial angular velocity vector of the i-th spacecraft with respect to an inertial frame $\mathscr{I}$ and expressed in the body-fixed frame $\mathscr{B}$. The attitude dynamics of the i-th spacecraft is given by[25,10]

$$\boldsymbol{J}_i\dot{\boldsymbol{\Omega}}_i = -\boldsymbol{\Omega}_i \times \boldsymbol{J}_i\boldsymbol{\Omega}_i + \boldsymbol{u}_i + \boldsymbol{d}_i \tag{8}$$

where $\boldsymbol{J}_i \in \mathbb{R}^{3\times3}, \boldsymbol{u}_i \in \mathbb{R}^3$ and $\boldsymbol{d}_i \in \mathbb{R}^3$ denote the symmetric positive definite inertia matrix in the body-fixed frame and the control torque, and the external disturbance of the i-th spacecraft, respectively.

Assumption 1. The external disturbance $\boldsymbol{d}_i$ of each spacecraft is bounded by an unknown positive constant $d_{i,\max}$, i.e., $\|\boldsymbol{d}_i\| \leqslant d_{i,\max}$. In addition, $d_{i,\max}$ is bounded by a known empirical value $D_{i,\max}$, i.e., $\|\boldsymbol{d}_i\| \leqslant d_{i,\max} < D_{i,\max}$, where $\| * \|$ denotes the Euclidean norm.

In addition, the actuators saturation is also considered in this work. The saturated control input $\boldsymbol{u}_i = [u_{i,1}, u_{i,2}, u_{i,3}]^{\mathrm{T}} \in \mathbb{R}^3$ in Eq. (8) is defined as $u_{i,p} = \mathrm{sign}(u_{i,p})\min(u_{i,\mathrm{sat},p}, |u_{i,p}|)$,[27] where $u_{i,p}$ and $u_{i,p,\mathrm{sat}}$ are the nominal input and saturation limit of the p-th actuator of the spacecraft with $p = 1, 2, 3$. The nonlinear saturation $\boldsymbol{u}_i$ in this work is approximately modeled as $\bar{\boldsymbol{u}}_i = [\bar{u}_{i,1}, \bar{u}_{i,2}, \bar{u}_{i,3}]^{\mathrm{T}} \in \mathbb{R}^3$ by using a dead-zone based model[28,29] with the relation

$$\bar{u}_{i,p} = \rho_{i,p,0}u_{i,p} - \int_0^{K_{i,p}} \rho_{i,p}(k)\mathscr{Z}(k, u_{i,p})\mathrm{d}k \tag{9}$$

where $\rho_{i,p}(k)$ is a known density function and is given as

$$\rho_{i,p}(k) = \begin{cases} \frac{2}{K_{i,p}} & k \leqslant K_{i,p} \\ 0 & k > K_{i,p} \end{cases} \tag{10}$$

The dead-zone operator

$$\mathscr{Z}(k, u_{i,p}) = \max\left(u_{i,p} - k, \min(0, u_{i,p} + k)\right) \tag{11}$$

Meanwhile, $\rho_{i,p,0} = \int_0^{K_{i,p}} \rho_{i,p}(k)\mathrm{d}k$ is a positive known constant parameter. We further have $u_{i,p,\mathrm{sat}} = K_{i,p}$ from $\rho_{i,p}(k)$.[22]

Then, the attitude dynamics of the i-th spacecraft Eq. (8) can be rewritten as

$$\boldsymbol{J}_i\dot{\boldsymbol{\Omega}}_i = -\boldsymbol{\Omega}_i \times \boldsymbol{J}_i\boldsymbol{\Omega}_i + \bar{\boldsymbol{u}}_i + \boldsymbol{d}_i \tag{12}$$

with

$$\bar{\boldsymbol{u}}_i = \boldsymbol{\rho}_{i,p,0} \circ \boldsymbol{u}_i - \boldsymbol{l}_i \tag{13}$$

where $\boldsymbol{\rho}_{i,p,0} = [\rho_{i,1,0}, \rho_{i,2,0}, \rho_{i,3,0}]^{\mathrm{T}} \in \mathbb{R}^3, \boldsymbol{l}_i = [l_{i,1}, l_{i,1}, l_{i,1}]^{\mathrm{T}} \in \mathbb{R}^3$ with $l_{i,p} = \int_0^{K_{i,p}} \rho_{i,p}(k)\mathscr{Z}(k, u_{i,p})dk, p = 1, 2, 3$. $\boldsymbol{u}_i = [u_{i,1}, u_{i,2}, u_{i,3}]^{\mathrm{T}} \in \mathbb{R}^3$ represents the controller output to be designed and the symbol $\circ$ denotes Hadamard product.

2.2. Stochastic process

The change of a stochastic variable in time can be expressed by a stochastic process $X = \{X(t), t \geqslant 0\}$. Let $\mathbb{P}\{\cdot\}$ and $\mathbb{E}\{\cdot\}$ denote the probability and the expected value of a stochastic variable. The conditional expected value of X given an event H is expressed by $\mathbb{E}\{X|H\}$. The stochastic process can be described by the probability triple $(\omega, \mathscr{F}, \mathbb{P})$,[30] where $\omega, \mathscr{F}$ and $\mathbb{P}$ are the space of events, a σ-algebra onto a subspace of ω, and the probability measure on $(\omega, \mathscr{F})$ with $0 \leqslant \mathbb{P}\{\cdot\} \leqslant 1$ and $\mathbb{P}\{\omega\} = 1$, respectively. In addition, a filtration $\{\mathscr{F}_t, t \geqslant 0\}$ on $(\omega, \mathscr{F}, \mathbb{P})$ is defined as a set of sub σ-algebras of $\mathscr{F}$ and satisfies $\mathscr{F}_s \subset \mathscr{F}_t (s < t)$.

In this condition, if $X(t)$ is $\mathscr{F}_t$-measurable for all $t \geqslant 0$, then the stochastic process $X = \{X(t), t \geqslant 0\}$ is adapted to the filtration $\{\mathscr{F}_t\}$. Moreover, a stochastic process X is a super-martingale relative to $\{\mathscr{F}_t\}$ and $\mathbb{P}$ if the following conditions are satisfied:[31]

(1) X is adapted to the filtration $\{\mathscr{F}_t\}$
(2) $\mathbb{E}\{|X(t)|\} < \infty \ \forall t$
(3) $\mathbb{E}\{X(t)|\mathscr{F}_s\} \leqslant X(s) \ t > s$

The stochastic variable $X(t)$ almost surely (a.s.) converges to a finite X_{f} if $\mathbb{P}\{\lim_{t\to\infty} X(t) = X_{\mathrm{f}}\} = 1$, which is further equivalently written as $\lim_{t\to\infty} X(t) \xrightarrow{\text{a.s.}} X_{\mathrm{f}}$.

Now, we can summarize the following super-martingale convergence lemma for deriving the main result of this paper:[32,24]

Lemma 1. If the stochastic process $X = \{X(t), t \geqslant 0\}$ is a nonnegative super-martingale, then there exists a finite X_{f} such that $\lim_{t\to\infty} X(t) \xrightarrow{\text{a.s.}} X_{\mathrm{f}}$.

2.3. Graph theory

The information topology between the leader spacecraft and the follower N spacecraft can be described by a directed graph $\mathscr{G} = (\mathscr{V}, \mathscr{E})$,[33] where $\mathscr{V} = \{1, 2, \cdots, N\}$ denotes the node set and $\mathscr{E} \subset \mathscr{V} \times \mathscr{V}$ is the edge set. The associated adjacency matrix is defined as $\mathscr{A} = [\alpha_{ij}] \in \mathbb{R}^{N\times N}$, where $\alpha_{ij} = 1$ if (i,j) is one element of $\mathscr{E}$, i.e., the mode i sends information to the node j, and $\alpha_{ij} = 0$ otherwise. Since there is no self-loop for each node in this work, $\alpha_{ii} = 0$ holds. The set of in-neighbors of the node i is denoted by $\mathscr{N}_i = \{j|(j,i) \in \mathscr{E}\}$. The in-degree matrix of the graph $\mathscr{G}$ is denoted by $\mathscr{D} = \mathrm{diag}(\mathscr{D}_1, \mathscr{D}_2, \ldots, \mathscr{D}_N)$, where $\mathscr{D}_i = \sum_{j\in\mathscr{N}_i}\alpha_{ij}$. The out-neighbors set of the node i is denoted by $\mathscr{O}_i = \{j|(i,j) \in \mathscr{E}\}$. The out-degree matrix of the graph $\mathscr{G}$ is denoted by $\mathscr{Q} = \mathrm{diag}(\mathscr{Q}_1, \mathscr{Q}_2, \ldots, \mathscr{Q}_N)$, where $\mathscr{Q}_i = \sum_{j\in\mathscr{O}_i}\alpha_{ji}$. Note that $\mathscr{D}_i$ indicates the number of nodes (except the leader) sending information to the node i and $\mathscr{Q}_i$ indicates the number of nodes (except the leader) receiving information from the node i. To describe the information flow from the virtual leader (i.e., node 0) to the followers, the leader adjacency matrix is defined as a diagonal matrix $\mathscr{B} = \mathrm{diag}(b_1, b_2, \ldots, b_N)$, where $b_i = 1$ if the

Uncorrected Proof

virtual leader sends information to node i, and $b_i = 0$ otherwise.

2.4. Communication links failure

In practical situations, the connectivity of communication links among spacecraft is vulnerable to indeterministic failures due to malicious attacks, environmental disturbances and randomly lost package of data, causing that the communication links may break off and reconstruct stochastically.

To model the random connectivity of the communication links for each node, two time-varying connection probabilities $p_{i,j}(t) \in (0,1]$ and $p_{i,0}(t) \in (0,1]$ are used, which describe the connectivity of the links from spacecraft $j \in \{1,2,\ldots,N\}$ satisfying $(j,i) \in \mathscr{E}$ and the virtual leader 0 to spacecraft $i \in \{1,2,\ldots,N\}$, respectively. It is noted that the communication link from the j-th spacecraft (or the virtual leader) to the i-th spacecraft cannot be disconnected all the time, i.e., $\forall t, p_{i,j}(t) \neq 0$ $(p_{i,0}(t) \neq 0)$. Otherwise, $\forall t, p_{i,j}(t) = 0$ $(p_{i,0}(t) = 0)$, the communication between the two spacecraft is always disconnected. In this case, the continuous links failure becomes deterministic, which is not within our consideration. Moreover, two stochastic switching parameters $a_{i,j}(p_{i,j})$ and $a_{i,0}(p_{i,0})$ associated with $p_{i,j}(t)$ and $p_{i,0}(t)$ for the i-th spacecraft are defined as

$$a_{i,j}(p_{i,j}) = \begin{cases} 1 & \text{with probability} p_{i,j}(t) \\ 0 & \text{with probability} 1 - p_{i,j}(t) \end{cases} \tag{14}$$

$$a_{i,0}(p_{i,0}) = \begin{cases} 1 & \text{with probability} p_{i,0}(t) \\ 0 & \text{with probability} 1 - p_{i,0}(t) \end{cases} \tag{15}$$

which indicate that the connection status of the communication link from the j-th spacecraft (or the virtual leader) to spacecraft i is nondeterministic and is with probability $p_{i,j}(t)$ (or $p_{i,0}(t)$) over time. Specifically, in Eq. (14), $a_{i,j}(p_{i,j}) = 1$ means that with probability $p_{i,j}(t)$ spacecraft j transmits information to spacecraft i at time t, while $a_{i,j}(p_{i,j}) = 0$ implies that with probability $1 - p_{i,j}(t)$ the communication link from spacecraft j to spacecraft i is disconnected at time t. Then, we can get the expectations of $a_{i,j}(p_{i,j})$ and $a_{i,0}(p_{i,0})$ for each link related to spacecraft i at time t, which are $\mathbb{E}\{a_{i,j}(p_{i,j})\} = p_{i,j}(t)$ and $\mathbb{E}\{a_{i,0}(p_{i,0})\} = p_{i,0}(t)$.

Next, define the following probability vector:

$$\boldsymbol{P}_i(t) \triangleq \left[p_{i,j_1}(t), \ldots, p_{i,j_k}(t), \ldots, p_{i,j_{\mathscr{D}_i}}(t), p_{i,0}(t)\right]^{\mathrm{T}} \tag{16}$$

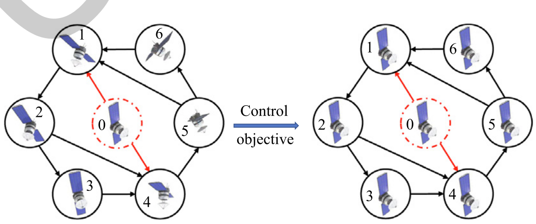

Fig. 1 Schematic diagram of control objective: Formation reaches an attitude consensus and attitude stabilization.

with $L_i = \mathscr{D}_i + b_i$ $\forall i \in \{1,2,\ldots,N\}$ and $(j_k, i) \in \mathscr{E}$ $\forall k \in \{1,2,\ldots,\mathscr{D}_i\}$. Then, the following assumptions are made about the connectivity probabilities.

Assumption 2. As $t \to \infty$, there exist $t_{i,1}, t_{i,2}, \cdots, t_{i,L_i}$ time instances for all $i \in \{1,2,\ldots,N\}$ such that the time-concatenated vectors of each element in $\boldsymbol{P}_i(t)$ are linearly independent. That is, the vectors

$$\underbrace{\begin{bmatrix} p_{i,j_1}(t_{i,1}) \\ p_{i,j_1}(t_{i,2}) \\ \vdots \\ p_{i,j_1}(t_{i,L_i}) \end{bmatrix}, \begin{bmatrix} p_{i,j_2}(t_{i,1}) \\ p_{i,j_2}(t_{i,2}) \\ \vdots \\ p_{i,j_2}(t_{i,L_i}) \end{bmatrix}, \ldots, \begin{bmatrix} p_{i,j_{\mathscr{D}_i}}(t_{i,1}) \\ p_{i,j_{\mathscr{D}_i}}(t_{i,2}) \\ \vdots \\ p_{i,j_{\mathscr{D}_i}}(t_{i,L_i}) \end{bmatrix}, \begin{bmatrix} p_{i,0}(t_{i,1}) \\ p_{i,0}(t_{i,2}) \\ \vdots \\ p_{i,0}(t_{i,L_i}) \end{bmatrix}}_{L_i \text{vectorsandeachoneisa} L_i \times 1 \text{vector}} \tag{17}$$

are linearly independent.

According to Assumption 2, the condition

$$\begin{aligned} &\beta_{i,1}\begin{bmatrix} p_{i,j_1}(t_{i,1}) \\ p_{i,j_1}(t_{i,1}) \\ \vdots \\ p_{i,j_1}(t_{i,L_i}) \end{bmatrix} + \beta_{i,2}\begin{bmatrix} p_{i,j_2}(t_{i,1}) \\ p_{i,j_2}(t_{i,2}) \\ \vdots \\ p_{i,j_2}(t_{i,L_i}) \end{bmatrix} + \cdots \\ &+\beta_{i,L_i-1}\begin{bmatrix} p_{i,j_{\mathscr{D}_i}}(t_{i,1}) \\ p_{i,j_{\mathscr{D}_i}}(t_{i,2}) \\ \vdots \\ p_{i,j_{\mathscr{D}_i}}(t_{i,L_i}) \end{bmatrix} + \beta_{i,L_i}\begin{bmatrix} p_{i,0}(t_{i,1}) \\ p_{i,0}(t_{i,2}) \\ \vdots \\ p_{i,0}(t_{i,L_i}) \end{bmatrix} = 0 \end{aligned} \tag{18}$$

holds as $t \to \infty$for each spacecraft i only when $\beta_{i,1} = \beta_{i,2} = \cdots = \beta_{i,L_i} = 0$.

Example 1. To illustrate the rationality of Assumption 2, the following example is given. Considering the communication topology shown in Fig. 1, for the spacecraft 1, there are two other spacecraft sending information to it, i.e., $\mathscr{D}_1 = 2$, and it also has communication with the virtual leader spacecraft, i.e., $L_1 = \mathscr{D}_1 + b_1 = 3$. Assuming that the connectivity of communication links for spacecraft 1 is with probabilities $p_{1,5}(t) = 0.8 + 0.1\cos(t/8), p_{1,6}(t) = 0.7 + 0.2\cos(t/5)$ and $p_{1,0}(t) = 0.9 - 0.1\sin(t/20)$. Taking any $L_1 = 3$ time instances, such as $t_{1,1} = 20$ s, $t_{1,2} = 50$ s, $t_{1,3} = 120$ s, we have vectors,

$$\begin{aligned} v_1 &= \begin{bmatrix} p_{1,5}(20) \\ p_{1,5}(50) \\ p_{1,5}(120) \end{bmatrix} = \begin{bmatrix} 0.7199 \\ 0.8999 \\ 0.7240 \end{bmatrix} \\ v_2 &= \begin{bmatrix} p_{1,6}(20) \\ p_{1,6}(50) \\ p_{1,6}(120) \end{bmatrix} = \begin{bmatrix} 0.5693 \\ 0.5322 \\ 0.7848 \end{bmatrix} \\ v_3 &= \begin{bmatrix} p_{1,0}(20) \\ p_{1,0}(50) \\ p_{1,0}(120) \end{bmatrix} = \begin{bmatrix} 0.8460 \\ 0.9801 \\ 0.8040 \end{bmatrix} \end{aligned} \tag{19}$$

Obviously, v_1, v_2 and v_3 are linearly independent and satisfy Assumption 2. It can be concluded that any two links can meet

Uncorrected Proof

Assumption 2 as long as the links failure probabilities are not equal.

Remark 1. In this work, the failure probability of any communication link varies over time t, and the failure probability of any two communication links is not always equal. Assumption 1 and its detailed illustration Example 1 further show the application range of stochastic links failure in this work, i.e., the failure probability of any two communication links is not equal at all times, otherwise, Assumption 1 is violated.

3. Problem statement

The objective of this paper is to design an attitude control scheme for an MSS with N spacecraft on SO(3) subject to stochastic communication failure, so that attitude consensus and the attitude stabilization can be achieved. In this work, we consider that spacecraft in the MSS are connected in a directed topology, and a virtual leader spacecraft provides the static desired attitude $\boldsymbol{R}_0$ for the MSS.

For example, as shown in Fig. 1, the virtual leader is only connected to the first and the fourth spacecraft in the topology. It is supposed that there is no isolated node in the communication graph, i.e., $\mathcal{N}_i \neq \varnothing \forall i$, and the information of the virtual leader spacecraft can be transmitted to any spacecraft through a directed path(s). In addition, we assume that each communication link between two spacecraft including the leader is not deterministic and may experience connection failure and reconstruction randomly over time.

This work mainly solves the following problem:

Problem 1. Under the stochastic links failure and actuator saturation, design a controller for the MSS on SO(3) with a static virtual leader to realize attitude consensus and attitude stabilization.

4. Attitude error function and dynamics

In this section, the attitude error function and the attitude error dynamic of a MSS based on SO(3) suitable for a directed topology link and with a static virtual leader are derived.

4.1. Attitude error function on SO(3)

The attitude error function on SO(3) of MSS is given in the following proposition.[25,10,34]

Proposition 1. For the i-th spacecraft, define an attitude error function $\Psi_i \in \mathbb{R}$, an attitude consensus error function $\Psi_{\mathrm{c},i} \in \mathbb{R}$, an attitude stabilization error function $\Psi_{\mathrm{s},i} \in \mathbb{R}$, an attitude consensus error vector $\boldsymbol{e}_{\mathrm{c},i} \in \mathbb{R}^3$, an attitude stabilization error vector $\boldsymbol{e}_{\mathrm{s},i} \in \mathbb{R}^3$, and an angular velocity error vector $\boldsymbol{e}_{\boldsymbol{\Omega},i} \in \mathbb{R}^3$ as follows:

$$\Psi_i = \sum_{j \in \mathcal{N}_i} \Psi_{\mathrm{c},i} + \Psi_{\mathrm{s},i} \tag{20}$$

$$\Psi_{\mathrm{c},i} = \frac{1}{2}\mathrm{tr}\left[\boldsymbol{I}_3 - \boldsymbol{R}_j^{\mathrm{T}}\boldsymbol{R}_i\right] \quad \forall j \in \mathcal{N}_i \tag{21}$$

$$\Psi_{\mathrm{s},i} = b_i\left(\frac{1}{2}\mathrm{tr}\left[\boldsymbol{I}_3 - \boldsymbol{R}_0^{\mathrm{T}}\boldsymbol{R}_i\right]\right) \tag{22}$$

$$\boldsymbol{e}_{\mathrm{c},i} = \frac{1}{2}\left(\boldsymbol{R}_j^{\mathrm{T}}\boldsymbol{R}_i - \boldsymbol{R}_i^{\mathrm{T}}\boldsymbol{R}_j\right)^{\vee} \quad \forall j \in \mathcal{N}_i \tag{23}$$

$$\boldsymbol{e}_{\mathrm{s},i} = \frac{1}{2}b_i\left(\boldsymbol{R}_0^{\mathrm{T}}\boldsymbol{R}_i - \boldsymbol{R}_i^{\mathrm{T}}\boldsymbol{R}_0\right)^{\vee} \tag{24}$$

$$\boldsymbol{e}_{\boldsymbol{\Omega},i} = \boldsymbol{\Omega}_i - b_i\boldsymbol{R}_i^{\mathrm{T}}\boldsymbol{R}_0\boldsymbol{\Omega}_0 = \boldsymbol{\Omega}_i \tag{25}$$

where $\boldsymbol{\Omega}_0 = \boldsymbol{0}$ is used in Eq. (25), because the virtual leader provides a static desired attitude. Subscripts i and j are the indexes indicating the i-th and j-th $(i, j \in \{1, 2 \cdots N\}, i \neq j)$ spacecraft in the MSS, respectively. Subscript 0 represents the virtual leader spacecraft.

Then, we can get the following properties:

(1) $\Psi_{\mathrm{c},i}, \Psi_{\mathrm{s},i}$ and Ψ_i are positive semi-definite and their zeros are at $\boldsymbol{R}_i = \boldsymbol{R}_j, \boldsymbol{R}_i = \boldsymbol{R}_0$ and $\boldsymbol{R}_i = \boldsymbol{R}_j = \boldsymbol{R}_0$, respectively.

(2) The left-trivialized derivatives of $\Psi_{\mathrm{c},i}, \Psi_{\mathrm{s},i}$ and Ψ_i with respect to the infinitesimal variation $\delta\boldsymbol{R}_i = \boldsymbol{R}_i\hat{\boldsymbol{\eta}}$ for $\boldsymbol{\eta} \in \mathbb{R}^3$ are given by

$$\mathrm{D}_{\boldsymbol{R}_i}\Psi_{\mathrm{c},i} \cdot \delta\boldsymbol{R}_i = \sum_{j \in \mathcal{N}_i} \boldsymbol{\eta}^{\mathrm{T}}\boldsymbol{e}_{\mathrm{c},i} \tag{26}$$

$$\mathrm{D}_{\boldsymbol{R}_i}\Psi_{\mathrm{s},i} \cdot \delta\boldsymbol{R}_i = \boldsymbol{\eta}^{\mathrm{T}}\boldsymbol{e}_{\mathrm{s},i} \tag{27}$$

$$\mathrm{D}_{\boldsymbol{R}_i}\Psi_i \cdot \delta\boldsymbol{R}_i = \sum_{j \in \mathcal{N}_i} \boldsymbol{\eta}^{\mathrm{T}}\boldsymbol{e}_{\mathrm{c},i} + \boldsymbol{\eta}^{\mathrm{T}}\boldsymbol{e}_{\mathrm{s},i} \tag{28}$$

(3) The defined errors $\boldsymbol{e}_{\mathrm{c},i}$ and $\boldsymbol{e}_{\mathrm{s},i}$ are bounded by

$$0 \leqslant \left\|\boldsymbol{e}_{\mathrm{c},i}\right\| \leqslant 1 \tag{29}$$

$$0 \leqslant \left\|\boldsymbol{e}_{\mathrm{s},i}\right\| \leqslant b_i \tag{30}$$

Proof. According to Rodrigues function, for any $\boldsymbol{Q} = \boldsymbol{R}_j^{\mathrm{T}}\boldsymbol{R}_i \in \mathrm{SO}(3)$, there exists $\boldsymbol{n} \in \mathbb{R}^3$ with $\|\boldsymbol{n}\| \leqslant \pi$ such that

$$\boldsymbol{Q} = \exp(\hat{\boldsymbol{n}}) = \boldsymbol{I}_3 + \frac{\sin\|\boldsymbol{n}\|}{\|\boldsymbol{n}\|}\hat{\boldsymbol{n}} + \frac{1 - \cos\|\boldsymbol{n}\|}{\|\boldsymbol{n}\|^2}\hat{\boldsymbol{n}}^2 \tag{31}$$

Substituting the foregoing equation into Eq. (21), we can obtain

$$\Psi_{\mathrm{c},i}\left(\boldsymbol{R}_j\exp(\hat{\boldsymbol{n}}), \boldsymbol{R}_j\right) = 1 - \cos(\|\boldsymbol{n}\|) \tag{32}$$

Therefore, it is clear that $0 \leqslant \Psi_{\mathrm{c},i} \leqslant 2$ and $\Psi_{\mathrm{c},i} = 0$ when $\boldsymbol{R}_i = \boldsymbol{R}_j$. Similarly, we can get $0 \leqslant \Psi_{\mathrm{s},i} \leqslant 2b_i$ and $\Psi_{\mathrm{s},i} = 0$ when $\boldsymbol{R}_i = \boldsymbol{R}_0$ or $b_i = 0$ indicating that the i-th spacecraft is not connected to the virtual leader spacecraft.

Because Ψ_i is the addition of $\Psi_{\mathrm{c},i}$ and $\Psi_{\mathrm{s},i}, \Psi_i$ is also positive definite about $\boldsymbol{R}_i = \boldsymbol{R}_j = \boldsymbol{R}_0$, and $\boldsymbol{R}_i = \boldsymbol{R}_j = \boldsymbol{R}_0$ is the critical point of Ψ_i. These show the above property (1).

The infinitesimal variation of a rotation matrix can be written as $\delta\boldsymbol{R} = \frac{\mathrm{d}}{\mathrm{d}\epsilon}\big|_{\epsilon=0}\boldsymbol{R}\exp(\epsilon\hat{\boldsymbol{\eta}}) = \boldsymbol{R}\hat{\boldsymbol{\eta}}$ for $\boldsymbol{\eta} \in \mathbb{R}^3$.[25] By lever-

Uncorrected Proof

aging this, the left-trivialized derivative of $\Psi_{c,i}$ with respect to $\boldsymbol{R}_i$ is given by

$$\begin{aligned} \mathrm{D}_{\boldsymbol{R}_i}\Psi_{c,i}\cdot\delta\boldsymbol{R}_i &= \frac{\mathrm{d}}{\mathrm{d}\epsilon}\Big|_{\epsilon=0}\Psi\left(\boldsymbol{R}_i(\exp\epsilon\hat{\boldsymbol{\eta}}),\boldsymbol{R}_j\right) \\ &= -\frac{1}{2}\mathrm{tr}\left[\boldsymbol{R}_j^T\boldsymbol{R}_i\hat{\boldsymbol{\eta}}\right] \end{aligned} \tag{33}$$

Using Eq. (4), $\mathrm{D}_{\boldsymbol{R}_i}\Psi_{c,i}\cdot\delta\boldsymbol{R}_i=\boldsymbol{\eta}^{\mathrm{T}}\boldsymbol{e}_{c,i}$ is further obtained. Similarly, we can also have $\mathrm{D}_{\boldsymbol{R}_i}\Psi_{s,i}\cdot\delta\boldsymbol{R}_i=\boldsymbol{\eta}^{\mathrm{T}}\boldsymbol{e}_{s,i}$ and $\mathrm{D}_{\boldsymbol{R}_i}\Psi_i\cdot\delta\boldsymbol{R}_i=\sum_{j\in\mathcal{N}_i}(\boldsymbol{\eta}^{\mathrm{T}}\boldsymbol{e}_{c,i})+\boldsymbol{\eta}^{\mathrm{T}}\boldsymbol{e}_{s,i}$. These show the above property (2).

Finally, substituting Eq. (31) into Eq. (23), we can obtain

$$\boldsymbol{e}_{c,i}=\frac{\sin\|\boldsymbol{n}\|}{\|\boldsymbol{n}\|}\boldsymbol{n} \tag{34}$$

Thus, $\|\boldsymbol{e}_{c,i}\|^2=\sin^2\|\boldsymbol{n}\|\leqslant 1$, which implies that $0\leqslant\|\boldsymbol{e}_{c,i}\|\leqslant 1$. Similarly, we can also obtain $0\leqslant\|\boldsymbol{e}_{s,i}\|\leqslant b_i$. These show the above property (3).

This completes the proof.

Remark 2. Proposition 1 defines an attitude consensus error function $\Psi_{c,i}$ and an attitude consensus error vector $\boldsymbol{e}_{c,i}$ to deal with the attitude consensus requirements of the i-th spacecraft and the j-th spacecraft in the MSS. An attitude stabilization error function $\Psi_{s,i}$ and an attitude stabilization error vector $\boldsymbol{e}_{s,i}$ are defined for the attitude stabilization requirements that each spacecraft stabilized to the desired attitude from the virtual leader spacecraft. The attitude error function Eq. (20) includes both attitude consensus error and attitude stabilization error, corresponding to the control objective of this work. The critical point of Ψ_i is $\boldsymbol{R}_i=\boldsymbol{R}_j=\boldsymbol{R}_0$, which ensures the realization of control objective. In addition, the parameter b_i in Ψ_i indicates whether the i-th spacecraft is connected to the virtual leader spacecraft, i.e., it determines whether the attitude stabilization requirements need to be considered for the i-th spacecraft.

Remark 3. Compared with the previous attitude error function of MSS[16,18,24] that only considers the attitude consensus error, an attitude error function including both attitude consensus error and attitude stabilization error on SO(3) is proposed in this work. Therefore, the proposed attitude error function Ψ_i in Eq. (20) can be applied for a directed topology link with a static virtual leader.

4.2. Attitude error dynamics on SO(3)

In this section, we derive the attitude error dynamics of the i-th spacecraft in the following proposition.

Proposition 2. The attitude error dynamics of the i-th spacecraft for the proposed $\Psi_i,\Psi_{c,i},\Psi_{s,i},\boldsymbol{e}_{c,i},\boldsymbol{e}_{s,i}$, and $\boldsymbol{e}_{\Omega,i}$ satisfy

$$\dot{\Psi}_i=\sum_{j\in\mathcal{N}_i}\dot{\Psi}_{c,i}+\dot{\Psi}_{s,i} \tag{35}$$

with

$$\dot{\Psi}_{c,i}=\left(\boldsymbol{\Omega}_i-\boldsymbol{R}_i^{\mathrm{T}}\boldsymbol{R}_j\boldsymbol{\Omega}_j\right)^{\mathrm{T}}\boldsymbol{e}_{c,i}\forall j\in\mathcal{N}_i \tag{36}$$

$$\dot{\Psi}_{s,i}=\boldsymbol{e}_{\Omega,i}^{\mathrm{T}}\boldsymbol{e}_{s,i} \tag{37}$$

$$\dot{\boldsymbol{e}}_{c,i}=\left(\mathrm{tr}\left[\boldsymbol{R}_i^{\mathrm{T}}\boldsymbol{R}_j\right]\boldsymbol{I}_3-\boldsymbol{R}_i^{\mathrm{T}}\boldsymbol{R}_j\right)\left(\boldsymbol{\Omega}_i-\boldsymbol{R}_i^{\mathrm{T}}\boldsymbol{R}_j\boldsymbol{\Omega}_j\right) \tag{38}$$

$$\dot{\boldsymbol{e}}_{s,i}=b_i\left(\mathrm{tr}\left[\boldsymbol{R}_i^{\mathrm{T}}\boldsymbol{R}_0\right]\boldsymbol{I}_3-\boldsymbol{R}_i^{\mathrm{T}}\boldsymbol{R}_0\right)\boldsymbol{e}_{\Omega,i} \tag{39}$$

$$\dot{\boldsymbol{e}}_{\Omega,i}=\boldsymbol{J}_i^{-1}\left(-\hat{\boldsymbol{\Omega}}_i\boldsymbol{J}_i\boldsymbol{\Omega}_i+\bar{\boldsymbol{u}}_i+\boldsymbol{d}_i\right) \tag{40}$$

Proof. For any desired attitude $\boldsymbol{R}_0\in\mathrm{SO}(3),\boldsymbol{R}_0^{\mathrm{T}}\boldsymbol{R}_0=\boldsymbol{I}_3$. Then, taking the time derivative on both sides results in $\dot{\boldsymbol{R}}_0^{\mathrm{T}}\boldsymbol{R}_0+\boldsymbol{R}_0^{\mathrm{T}}\dot{\boldsymbol{R}}_0=\boldsymbol{0}$, which further implies

$$\dot{\boldsymbol{R}}_0^{\mathrm{T}}=-\boldsymbol{R}_0^{\mathrm{T}}\dot{\boldsymbol{R}}_0\boldsymbol{R}_0^{\mathrm{T}}. \tag{41}$$

Then, in view of Eq. (41), the derivative of $\boldsymbol{R}_0^{\mathrm{T}}\boldsymbol{R}_i$ is obtained as

$$\begin{aligned} \boldsymbol{R}_0^{\mathrm{T}}\dot{\boldsymbol{R}}_i+\dot{\boldsymbol{R}}_0^{\mathrm{T}}\boldsymbol{R}_i &= \boldsymbol{R}_0^{\mathrm{T}}\left[\boldsymbol{R}_i\hat{\boldsymbol{\Omega}}_i-\boldsymbol{R}_0\hat{\boldsymbol{\Omega}}_0\left(\boldsymbol{R}_0^{\mathrm{T}}\boldsymbol{R}_i\right)\right] \\ &= \boldsymbol{R}_0^{\mathrm{T}}\boldsymbol{R}_i\left(\boldsymbol{\Omega}_i-\boldsymbol{R}_i^{\mathrm{T}}\boldsymbol{R}_0\boldsymbol{\Omega}_0\right)^{\wedge} \end{aligned} \tag{42}$$

where Eq. (6) is used. In addition, since the static task is considered, i.e., $\boldsymbol{\Omega}_0=\boldsymbol{0}$, it follows that

$$\boldsymbol{R}_0^{\mathrm{T}}\dot{\boldsymbol{R}}_i+\dot{\boldsymbol{R}}_0^{\mathrm{T}}\boldsymbol{R}_i=\boldsymbol{R}_0^{\mathrm{T}}\boldsymbol{R}_i\hat{\boldsymbol{\Omega}}_i \tag{43}$$

Following the above derivation, we can obtain

$$\boldsymbol{R}_j^{\mathrm{T}}\dot{\boldsymbol{R}}_i+\dot{\boldsymbol{R}}_j^{\mathrm{T}}\boldsymbol{R}_i=\boldsymbol{R}_j^{\mathrm{T}}\boldsymbol{R}_i\left(\boldsymbol{\Omega}_i-\boldsymbol{R}_i^{\mathrm{T}}\boldsymbol{R}_j\boldsymbol{\Omega}_j\right)^{\wedge} \tag{44}$$

Then, it is clear from Eq. (21) that

$$\begin{aligned} \dot{\Psi}_{c,i} &= -\frac{1}{2}\mathrm{tr}\left[\boldsymbol{R}_j^{\mathrm{T}}\dot{\boldsymbol{R}}_i+\dot{\boldsymbol{R}}_j^{\mathrm{T}}\boldsymbol{R}_i\right]=-\frac{1}{2}\mathrm{tr}\left[\boldsymbol{R}_j^{\mathrm{T}}\boldsymbol{R}_i\left(\boldsymbol{\Omega}_i-\boldsymbol{R}_i^{\mathrm{T}}\boldsymbol{R}_j\boldsymbol{\Omega}_j\right)^{\wedge}\right] \\ &= \left(\boldsymbol{\Omega}_i-\boldsymbol{R}_i^{\mathrm{T}}\boldsymbol{R}_j\boldsymbol{\Omega}_j\right)^{\mathrm{T}}\left(\boldsymbol{R}_j^{\mathrm{T}}\boldsymbol{R}_i-\boldsymbol{R}_i^{\mathrm{T}}\boldsymbol{R}_j\right)^{\vee} \end{aligned} \tag{45}$$

where the property given in Eq. (4) is used. Similarly, by leveraging Eq. (43) and Eq. (4), we can also show Eq. (37). Then, we show Eq. (37)

$$\begin{aligned} \dot{\boldsymbol{e}}_{c,i} =& \left(\boldsymbol{R}_j^{\mathrm{T}}\boldsymbol{R}_i\left(\boldsymbol{\Omega}_i-\boldsymbol{R}_i^{\mathrm{T}}\boldsymbol{R}_j\boldsymbol{\Omega}_j\right)^{\wedge}+\left(\boldsymbol{\Omega}_i-\boldsymbol{R}_i^{\mathrm{T}}\boldsymbol{R}_j\boldsymbol{\Omega}_j\right)^{\wedge}\boldsymbol{R}_i^{\mathrm{T}}\boldsymbol{R}_j\right)^{\vee} \\ =& \left(\mathrm{tr}\left[\boldsymbol{R}_i^{\mathrm{T}}\boldsymbol{R}_j\right]\boldsymbol{I}-\boldsymbol{R}_i^{\mathrm{T}}\boldsymbol{R}_j\right)\left(\boldsymbol{\Omega}_i-\boldsymbol{R}_i^{\mathrm{T}}\boldsymbol{R}_j\boldsymbol{\Omega}_j\right) \end{aligned} \tag{46}$$

where Eq. (44) and Eq. (5) are used. Similarly, by using Eq. (43) and Eq. (5), we can show Eq. (39).

Moreover, since the inertia matrix of each spacecraft is positive definite, according to Eq. (12), it is trivial to get Eq. (40).

This completes the proof.

5. Controller design

In this section, we solve Problem 1 by proposing an attitude controller approach for the MSS on SO(3) to achieve attitude consensus and attitude stabilization with the stochastic links failure.

In light of Eq. (36), Eq. (37) and Eq. (40), an attitude controller can be designed as

Uncorrected Proof

Please cite this article in press as: KANG Z et al. Attitude control of multi-spacecraft systems on SO(3) with stochastic links failure, *Chin J Aeronaut* (2023), https://doi.org/10.1016/j.cja.2023.12.019

$$\begin{aligned}\boldsymbol{u}_i = \ & \boldsymbol{\chi}\circ\Bigg(-k_1\sum_{j\in\mathcal{N}_i}a_{i,j}(p_{i,j})\boldsymbol{e}_{c,i}-k_2a_{i,0}(p_{i,0})\boldsymbol{e}_{s,i}\\ & -(k_3+k_4)\tfrac{\|\boldsymbol{\Omega}_i\|^2}{\|\boldsymbol{\Omega}_i\|+\kappa_i^2}+\boldsymbol{l}_i\Bigg)\end{aligned} \tag{47}$$

with

$$\dot{\kappa}=-\gamma_i\frac{(k_3+k_4)\kappa_i\|\boldsymbol{\Omega}_i\|}{\|\boldsymbol{\Omega}_i\|+\kappa_i^2} \tag{48}$$

where $\boldsymbol{\chi}=\left[\frac{1}{\rho_{i,1,0}},\frac{1}{\rho_{i,2,0}},\frac{1}{\rho_{i,3,0}}\right]^{\mathrm{T}}\in\mathbb{R}^3; k_1,k_2,k_3,k_4>D_{i,\max}$ and γ_i are positive constants.

Using the proposed attitude controller Eq. (47), the stability of the MSS is summarized as the following theorem.

Theorem 1. For the attitude error kinematics and dynamics on SO(3) represented by Eq. (35) and Eq. (40), the proposed attitude controller Eq. (47) and adaptive update law Eq. (48) with $k_3>\max\{k_1,k_2\}\mathscr{S}$ and $k_4>D_{i,\max}$, where $\mathscr{S}\triangleq 2\|\mathscr{D}\|_1+\|\mathscr{Q}\|_1+1$ ensures that the attitude of MSS can almost surely achieve consensus and stabilization despite stochastic links failure.

Proof. Consider the following Lyapunov candidate function:

$$V=\sum_{i=1}^{N}\left(\frac{1}{2}\boldsymbol{\Omega}_i^{\mathrm{T}}\boldsymbol{J}_i\boldsymbol{\Omega}_i+k_5\Psi_i+\frac{1}{\gamma_i}\kappa_i^2\right) \tag{49}$$

where $k_5=\max\{k_1,k_2\}$. Substituting the attitude dynamics Eq. (40) and the attitude controller Eq. (47) into the time derivative of V yields

$$\begin{aligned}\dot{V}\leqslant\sum_{i=1}^{N} & \Bigg(k_5\sum_{j\in\mathcal{N}_i}a_{i,j}(p_{i,j})\|\boldsymbol{e}_{c,i}\|\|\boldsymbol{\Omega}_i\|-(k_4-D_{i,\max})\|\boldsymbol{\Omega}_i\|\\ & +k_5(1-a_{i,0}(p_{i,0}))\|\boldsymbol{e}_{s,i}\|\|\boldsymbol{\Omega}_i\|-k_3\|\boldsymbol{\Omega}_i\|\\ & +k_5\sum_{j\in\mathcal{N}_i}\|\boldsymbol{e}_{c,i}\|\|\boldsymbol{\Omega}_i-\boldsymbol{R}_i^{\mathrm{T}}\boldsymbol{R}_j\boldsymbol{\Omega}_j\|\Bigg)\end{aligned} \tag{50}$$

where the fact $\boldsymbol{\Omega}_i^{\mathrm{T}}\hat{\boldsymbol{\Omega}}_i=0$ is used. Then, due to $\|\boldsymbol{R}_i^{\mathrm{T}}\boldsymbol{R}_j\|\leqslant 1$,

$$\|\boldsymbol{\Omega}_i-\boldsymbol{R}_i^{\mathrm{T}}\boldsymbol{R}_j\boldsymbol{\Omega}_j\|\leqslant\|\boldsymbol{\Omega}_i\|+\|\boldsymbol{\Omega}_j\| \tag{51}$$

Moreover, according to $\|\boldsymbol{e}_{c,i}\|\leqslant 1$ and $\|\boldsymbol{e}_{s,i}\|\leqslant b_i$ from Proposition 1 along with the fact that $b_i\in\{0,1\}, a_{i,j}(p_{i,j})\in\{0,1\}, a_{i,0}(p_{i,0})\in\{0,1\}$ and $\mathscr{D}_i=\sum_{j\in\mathcal{N}_i}\alpha_{ij}\leqslant\|\mathscr{D}\|_1$ where $\|\cdot\|_1$ represents the 1-norm of the matrix, it follows from Eq. (50) and Eq. (51) that

$$\begin{aligned}\dot{V}\leqslant & \sum_{i=1}^{N}\Bigg(k_5\sum_{j\in\mathcal{N}_i}[1+a_{i,j}(p_{i,j})]\|\boldsymbol{e}_{c,i}\|\|\boldsymbol{\Omega}_i\|+k_5\sum_{j\in\mathcal{N}_i}\|\boldsymbol{e}_{c,i}\|\|\boldsymbol{\Omega}_j\|\\ & -(k_3-k_5[1-a_{i,0}(p_{i,0})]\|\boldsymbol{e}_{s,i}\|)\|\boldsymbol{\Omega}_i\|\Bigg)\end{aligned} \tag{52}$$

Further, we can obtain

$$\begin{aligned}\dot{V}\leqslant & \sum_{i=1}^{N}\Bigg(2k_5\mathscr{D}_i\|\boldsymbol{\Omega}_i\|-(k_3-k_5)\|\boldsymbol{\Omega}_i\|+k_5\sum_{j\in\mathcal{N}_i}\|\boldsymbol{\Omega}_i\|\Bigg)\\ \leqslant & \sum_{i=1}^{N}(-[k_3-k_5(2\|\mathscr{D}\|_1+1)]\|\boldsymbol{\Omega}_i\|)+k_5\sum_{i=1}^{N}\sum_{j\in\mathcal{N}_i}\|\boldsymbol{\Omega}_j\|\end{aligned} \tag{53}$$

Recognizing that

$$\sum_{i=1}^{N}\sum_{j\in\mathcal{N}_i}\|\boldsymbol{\Omega}_j\|\leqslant\sum_{i=1}^{N}\|\mathscr{Q}\|_1\|\boldsymbol{\Omega}_i\| \tag{54}$$

we can substitute it into Eq. (53) and obtain

$$\dot{V}\leqslant-[k_3-k_5(2\|\mathscr{D}\|_1+\|\mathscr{Q}\|_1+1)]\sum_{i=1}^{N}\|\boldsymbol{\Omega}_i\| \tag{55}$$

As a consequence, if the control gains are selected to satisfy

$$k_4>D_{i,\max},\quad k_3>k_5\mathscr{S}>\max\{k_1,k_2\}\mathscr{S} \tag{56}$$

where $\mathscr{S}\triangleq 2\|\mathscr{D}\|_1+\|\mathscr{Q}\|_1+1$, we can obtain that $\dot{V}$ is negative semidefinite. Then, by invoking the generalized invariance principle for nonautonomous systems,[35,24] we can conclude

$$\lim_{t\to\infty}\boldsymbol{\Omega}_i\equiv\boldsymbol{0}_{3\times 1} \tag{57}$$

Thus, $\boldsymbol{\Omega}_i=0$ and $\dot{\boldsymbol{\Omega}}_i=0$ as $t\to\infty$

Then, substituting the conclusion into attitude error dynamics Eq. (40) and controller Eq. (47) yields

$$\sum_{j\in\mathcal{N}_i}a_{i,j}(p_{i,j})\boldsymbol{e}_{c,i}+a_{i,0}(p_{i,0})\boldsymbol{e}_{s,i}=\boldsymbol{0}_{3\times 1}\ t\to\infty \tag{58}$$

Considering that $a_{i,j}(p_{i,j})$ and $a_{i,0}(p_{i,0})$ are stochastic variables, computing expectations on both sides of Eq. (58) leads to

$$\sum_{j\in\mathcal{N}_i}p_{i,j}(t)\boldsymbol{e}_{c,i}+p_{i,0}\boldsymbol{e}_{s,i}=\boldsymbol{0}_{3\times 1} \tag{59}$$

as $t\to\infty$. In view of Eq. (38), Eq. (39) and Eq. (40, $\dot{\boldsymbol{e}}_{c,i}=\dot{\boldsymbol{e}}_{s,i}=\boldsymbol{0}_{3\times 1}$, i.e., as $t\to\infty, \boldsymbol{e}_{c,i}\in\mathbb{R}^3$ and $\boldsymbol{e}_{s,i}\in\mathbb{R}^3$ are constant vectors. According to Assumption 2, for the i-th spacecraft $\exists L_i=\mathscr{D}_i+b_i$ vectors and

$$\sum_{j\in\mathcal{N}_i}\left(\boldsymbol{e}_{c,i}(q)\begin{bmatrix}p_{i,j}(t_{i,1})\\p_{i,j}(t_{i,2})\\\vdots\\p_{i,j}(t_{i,L_i})\end{bmatrix}\right)+\boldsymbol{e}_{s,i}(q)\begin{bmatrix}p_{i,0}(t_{i,1})\\p_{i,0}(t_{i,2})\\\vdots\\p_{i,0}(t_{i,L_i})\end{bmatrix}=\boldsymbol{0}_{L\times 1} \tag{60}$$

where $\boldsymbol{X}(q)$ with $q=1,2,3$ represents the q-th number of $\boldsymbol{X}$. Then, by using the vector linear independence theorem, we can further obtain $\boldsymbol{e}_{c,i}\to\boldsymbol{0}_{3\times 1}, j\in\mathcal{N}_i$ and $\boldsymbol{e}_{s,i}\to\boldsymbol{0}_{3\times 1}$ as $t\to\infty$, which can be further expressed as

$$\begin{aligned}&\mathbb{P}\left\{\left\|\left(\boldsymbol{R}_j^{\mathrm{T}}\boldsymbol{R}_i-\boldsymbol{R}_i^{\mathrm{T}}\boldsymbol{R}_j\right)^{\vee}\right\|>\varepsilon_1\right\}=0\ \forall j\in\mathcal{N}_i,\ t\to\infty\\ &\mathbb{P}\left\{\left\|\left(\boldsymbol{R}_0^{\mathrm{T}}\boldsymbol{R}_i-\boldsymbol{R}_i^{\mathrm{T}}\boldsymbol{R}_0\right)^{\vee}\right\|>\varepsilon_2\right\}=0\ t\to\infty\end{aligned} \tag{61}$$

where ε_1 and ε_2 are any positive minimum. Then, by defining the filtration

$$\mathscr{F}_t=\left\{\left[\boldsymbol{R}_i(\varrho)^{\mathrm{T}},\boldsymbol{R}_j(\varrho)^{\mathrm{T}},\boldsymbol{\Omega}(\varrho)_i^{\mathrm{T}}\right],\ 0\leqslant\varrho\leqslant t\right\} \tag{62}$$

the following three conditions can be obtained:

(1) For the MSS, the Lyapunov

$$V(t)=\sum_{i=1}^{N}\left(\frac{1}{2}\boldsymbol{\Omega}_i^{\mathrm{T}}(t)\boldsymbol{J}_i\boldsymbol{\Omega}_i(t)+k_5\Psi_i(t)+\frac{1}{\gamma_i}\kappa_i^2(t)\right) \tag{63}$$

can be regarded as a stochastic process, and $V(t)$ is $\mathscr{F}_t$-measurable for any time t. Since $V(t)$ is determined by

Uncorrected Proof

$\boldsymbol{R}_i(\varrho), \boldsymbol{R}_j(\varrho)$, and $\boldsymbol{\Omega}(\varrho)_i$ as well as their history, $V(t)$ only depends on $\{\mathscr{F}_s, 0 \leqslant s \leqslant t\}$, and thus $V(t)$ is determined for the filtration $\mathscr{F}_t$.

(2) Given the result of the Lyapunov analysis $\dot{V}(t) \leqslant 0$, we have $\boldsymbol{R}_i(\varrho), \boldsymbol{R}_j(\varrho)$, and $\boldsymbol{\Omega}(\varrho)_i$ are bounded. Therefore, $V(t)$ is bounded. Thus, which $\mathbb{E}\{V(t)\}$ is also bounded.

(3) Since $\dot{V}(t) \leqslant 0$, we know $V(t) \leqslant V(s)$if $t \geqslant s$. In view of the fact that $V(t)$ is measurable for any t and according to the property of conditional expectation,

$$\mathbb{E}\{V(t)|\mathscr{F}_s\} = V(t) \leqslant V(s)\ t \geqslant s \tag{64}$$

As a consequence, the above three conditions yield that $V(t)$ is super-martingale. Then, according to Lemma 1, we know that

$$\lim_{t\to\infty} V(t) \to V_\mathrm{f} \tag{65}$$

where V_f is a nonnegative finite real number. From the Lyapunov function

$$V(t) = \sum_{i=1}^{N}\left(\frac{1}{2}\boldsymbol{\Omega}_i^\mathrm{T}(t)\boldsymbol{J}_i\boldsymbol{\Omega}_i(t) + k_5\Psi_i(t) + \frac{1}{\gamma_i}\kappa_i^2(t)\right) \tag{66}$$

and $t \to \infty$, $\boldsymbol{\Omega}_i = \boldsymbol{0}$, we have

$$\lim_{t\to\infty}\Psi_i \overset{\text{a.s.}}{\to} V_\mathrm{f}\ i = 1, 2, \cdots, N \tag{67}$$

Due to the fact that Ψ_i is positive definite about $\boldsymbol{R}_i = \boldsymbol{R}_j = \boldsymbol{R}_0$, and Eq. (61), we can conclude that $V_\mathrm{f} = 0$. Then, the critical point of Ψ_i is $\boldsymbol{R}_i = \boldsymbol{R}_j = \boldsymbol{R}_0$. Therefore,

$$\lim_{t\to\infty}\boldsymbol{R}_i \overset{\text{a.s.}}{\to} \boldsymbol{R}_j \overset{\text{a.s.}}{\to} \boldsymbol{R}_0, \forall i = 1, 2, \cdots, N \tag{68}$$

This is equivalent to

$$\mathbb{P}\left\{\lim_{t\to\infty}\boldsymbol{R}_i = \boldsymbol{R}_j = \boldsymbol{R}_0\right\} = 1 \quad \forall i = 1, 2, \cdots, N. \tag{69}$$

This implies that the spacecraft attitude in the MSS tends to be consistent, and stable at the desired attitude provided by the virtual leader spacecraft.

This completes the proof.

Remark 4. The gains k_1 and k_2 in controller Eq. (47) are equivalent to the proportional coefficient in a PD controller, and k_3 is equal to the derivative coefficient. The larger k_1 and k_2 are chosen, the faster the attitude error converges, but it will cause system oscillation, and it is necessary to increase k_3 at the same time. k_4 is the coefficient used to counteract external disturbances. Once the value $D_{i,\max}$ is determined based on experience, an appropriate value of k_4 can be selected. Therefore, we can select the appropriate values of k_1, k_2, k_3 and k_4 when condition Eq. (56) is satisfied.

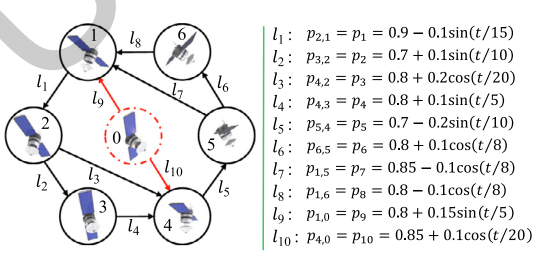

Fig. 2 Communication links between spacecraft with probability of successful connection.

Remark 5. The Eq. (59) is expressed as $\sum_{j\in\mathscr{N}_i} p_{i,j}(t)\boldsymbol{e}_{\mathrm{c},i} = \boldsymbol{0}_{3\times1}$ without item related to the virtual leader in the study of Rezaee and Abdollahi,[24] so the conclusion of $\boldsymbol{e}_{\mathrm{c},i} \to \boldsymbol{0}_{3\times1}, j \in \mathscr{N}_i$ as $t \to \infty$ can be obtained directly. The conclusion that $\boldsymbol{e}_{\mathrm{c},i} \to \boldsymbol{0}_{3\times1}, j \in \mathscr{N}_i$ and $\boldsymbol{e}_{\mathrm{s},i} \to \boldsymbol{0}_{3\times1}$ as $t \to \infty$ cannot be directly obtained by introducing the communication links related to the virtual leader. However, this work can draw this conclusion ($\boldsymbol{e}_{\mathrm{c},i} \to \boldsymbol{0}_{3\times1}, j \in \mathscr{N}_i$ and $\boldsymbol{e}_{\mathrm{s},i} \to \boldsymbol{0}_{3\times1}$ as $t \to \infty$) under Assumption 2, which is the most significant difference from Rezaee and Abdollahi.[24] Therefore, we can not only achieve the attitude consensus of MSS, but also achieve the attitude stabilization under stochastic links failure.

6. Simulation results

In this section, the effectiveness of the proposed attitude controller is demonstrated by numerical simulation for the MSS with stochastic links failure.

We consider a leader–follower MSS composed of six spacecraft and a virtual leader spacecraft in the numerical simulation. The communication links among spacecraft and the probability of successful connection of each link are shown in Fig. 2. Obviously, the connection probabilities $p_{i,j}(t) \in (0, 1]$ and $p_{i,0}(t) \in (0, 1]$ and the connectivity probabilities of all links satisfy Assumption 2 and $\|\mathscr{D}\|_1 = 2, \|\mathscr{Q}\|_1 = 2$.

To simulate the stochastic links failures, the following random numbers associated with each link are introduced:

$$\begin{aligned} c_{i,j} &= \mathrm{rand}(1)\ i \in \{1, 2, \cdots, 6\},\ j \in \mathscr{N}_i \\ c_{i,0} &= \mathrm{rand}(1)\ i \in \{1, 4\} \end{aligned} \tag{70}$$

where $\mathrm{rand}(1) \in [0, 1]$ is a random number. Then, the connectivity of each link can be expressed as

$$\begin{aligned} a_{i,j}(p_{i,j}) &= \begin{cases} 1 & c_{i,j} \leqslant p_{i,j} \\ 0 & c_{i,j} > p_{i,j} \end{cases},\ \begin{array}{l} i \in \{1, 2, \cdots, 6\} \\ \text{and} j \in \mathscr{N}_i \end{array} \\ a_{i,0}(p_{i,0}) &= \begin{cases} 1 & c_{i,0} \leqslant p_{i,0} \\ 0 & c_{i,0} > p_{i,0} \end{cases},\ i \in \{1, 4\} \end{aligned} \tag{71}$$

The inertia matrices of the MSS are given as

$$\boldsymbol{J}_i = \begin{bmatrix} 60 & 0 & -5 \\ 0 & 65 & 0 \\ -5 & 0 & 70 \end{bmatrix} \mathrm{kg}\cdot\mathrm{m}^2 \quad i = 1, 2, \cdots, 6 \tag{72}$$

The external disturbance of each spacecraft is

$$\boldsymbol{d}_i = 10^{-3} \times \begin{bmatrix} -1 + 3\cos(0.1it) + 4\sin(0.03it) \\ 1.5 - 1.5\sin(0.02it) - 3\cos(0.05it) \\ 1 + \sin(0.1it) - 1.5\cos(0.04it) \end{bmatrix} \mathrm{N}\cdot\mathrm{m} \tag{73}$$

where $i = 1, 2, \cdots, 6$. The saturation limit of the actuators of the i-th spacecraft is given as $u_{i,p,\mathrm{sat}} = 1$ N·m, $p = 1, 2, 3$, resulting in $\|\bar{\boldsymbol{u}}_i\| \leqslant \sqrt{3}$N·m.

The initial states of the MSS are given in Table 1, and the map$\boldsymbol{R} = \exp(\theta, \boldsymbol{n}) \to \mathrm{SO}(3)$ is defined as

$$\boldsymbol{R} = \exp(\theta, \boldsymbol{n}) = \boldsymbol{I}_3 + \sin(\theta)\hat{\boldsymbol{n}} + (1 - \cos(\theta))\hat{\boldsymbol{n}}^2 \tag{74}$$

In addition, the desired attitude $\boldsymbol{R}_0 = \boldsymbol{I}_3$, and the corresponding desired unit-quaternion $\boldsymbol{Q}_\mathrm{d} = \left[\boldsymbol{q}_\mathrm{d}^\mathrm{T}, q_\mathrm{d}\right]^\mathrm{T} = [0, 0, 0, 1]^\mathrm{T}$. In

Uncorrected Proof

Table 1 Initial states of MSS.

No.	$\boldsymbol{R}_i(0) = \exp(\theta_i(0), \boldsymbol{n}_i(0))$	$\boldsymbol{\Omega}_i(0)$ (rad/s)
1	$\theta_1(0) = -10^\circ, \boldsymbol{n}_1(0) = [0,0,1]^{\mathrm{T}}$	$[0.1, 0.05, -0.2]^{\mathrm{T}}$
2	$\theta_2(0) = 135^\circ, \boldsymbol{n}_2(0) = \frac{[0,1,1]^{\mathrm{T}}}{\|[0,1,1]\|}$	$[0, 0.06, 0.2]^{\mathrm{T}}$
3	$\theta_3(0) = 175^\circ, \boldsymbol{n}_3(0) = \frac{[1,0,1]^{\mathrm{T}}}{\|[1,0,1]\|}$	$[-0.1, 0.3, -0.05]^{\mathrm{T}}$
4	$\theta_4(0) = 70^\circ, \boldsymbol{n}_4(0) = [0,1,0]^{\mathrm{T}}$	$[-0.03, 0.5, -0.2]^{\mathrm{T}}$
5	$\theta_5(0) = 225^\circ, \boldsymbol{n}_5(0) = [1,0,0]^{\mathrm{T}}$	$[0.3, 0, -0.2]^{\mathrm{T}}$
6	$\theta_6(0) = -80^\circ, \boldsymbol{n}_6(0) = \frac{[1,1,0]^{\mathrm{T}}}{\|[1,1,0]\|}$	$[-0.1, -0.1, 0]^{\mathrm{T}}$

	A B	C D	E F	G H	X Y	N M
Case No.	500 s	750 s	500 s	750 s	500 s	750 s
Case 1	1	2	3	4	5	6
Case 1	7	8	9	10	11	12
Case 1	13	14	15	16	17	18

addition, the unit-quaternion attitude consensus error is computed as $\boldsymbol{Q}_{\mathrm{c,e},i} = \left[\boldsymbol{q}_{\mathrm{c,e},i}^{\mathrm{T}}, q_{\mathrm{c,e},i}\right]^{\mathrm{T}} = \sum_{j\in\mathcal{N}_i} \boldsymbol{Q}_j^* \otimes \boldsymbol{Q}_i$, where $\otimes$ is the quaternion multiplication operator,[36] $\boldsymbol{Q}_i$ is the current attitude of the i-th spacecraft. The unit-quaternion attitude stabilization error is computed as $\boldsymbol{Q}_{\mathrm{s,e},i} = \left[\boldsymbol{q}_{\mathrm{s,e},i}^{\mathrm{T}}, q_{\mathrm{s,e},i}\right]^{\mathrm{T}} = \boldsymbol{Q}_{\mathrm{d}}^* \otimes \boldsymbol{Q}_i$. Next, we consider two parts of numerical simulation to illustrate the performance of the proposed controller Eq. (47) under different stochastic links modeling methods.

6.1. Comparison of different control situations

In this subsection, the proposed controller based on SO(3) for a leader–follower MSS and the existing controller based on unit-quaternion for a leaderless MSS in the study of Rezaee and Abdollahi[24] are compared to illustrate that the proposed one can avoid fuzziness of unit-quaternion and reach the desired attitude. Three control situations are considered.

Situation 1. The proposed controller Eq. (47) is applied to the SO(3)-based leader–follower MSS with stochastic links failure. In this control situation, we set $k_1 = k_2 = 10.5, k_3 = 150$ to meet the condition Eq. (56).

Situation 2. The attitude consensus controller (4) in the study of Rezaee and Abdollahi[24] acts on a leaderless MSS using the unit-quaternion with stochastic links failure. The control parameters are set as $\gamma = 10.5$ and $k_i = 150$.

Situation 3. It is the same with Situation 2, but the initial unit-quaternions $\boldsymbol{Q}_i(0)$ of the Spacecrafts $1, 3, 4$ and 6 are changed to $-\boldsymbol{Q}_i(0)$ ($\boldsymbol{Q}_i(0)$ and $-\boldsymbol{Q}_i(0)$ are the same attitude).

In this subsection, the stochastic links failure in the three situations of interest may occur at each sampling instance with a sampling period $T_{\mathrm{step}} = 0.02$ s, i.e., random numbers $c_{i,j}$ or $c_{i,0}$ are generated at each sampling instance to determine the connectivity of the communication links according to Eq. (71).

Figs. 3–5 show the time history of attitude consensus error, attitude stabilization error, angular velocity and control torque under different modeling methods of MSS, respectively. For the leader–follower MSS on SO(3), the proposed controller Eq. (47) can achieve attitude consensus and attitude stabilization, where the attitude consensus is completed in 150 s with steady-state error $\Psi_{\mathrm{c},i} \leqslant 5 \times 10^{-6}$, as shown in Fig. 3(a). The attitude stabilization is completed in 300 s with steady-state error $\Psi_{\mathrm{s},i} \leqslant 3 \times 10^{-5}$, as shown in Fig. 3(b). Moreover, the angular velocity $\|\boldsymbol{\Omega}_i\|$, as shown in Fig. 3(c), tends to be stable at 300 s with the steady-state error $\|\boldsymbol{\Omega}_i\| \leqslant 5 \times 10^{-3}$ °/s. In addition, it can be seen from the controller Eq. (47) that considering the stochastic links failure, $a_{i,j}(p_{i,j})$ and $a_{i,0}(p_{i,0})$ have a probability of 1 or 0, which sometimes leads to the absence of the attitude consistency error $\boldsymbol{e}_{\mathrm{c},i}$ and the attitude stabilization error $\boldsymbol{e}_{\mathrm{s},i}$, which further leads to the jump fluctuation of the controller output, as observed in Fig. 3(d).

From Fig. 3(d) and Fig. 5(a), the controller (4) in the study of Rezaee and Abdollahi[24] can achieve attitude consensus under stochastic links failure. Since the controller (4) in the study of Rezaee and Abdollahi[24] is only applicable to the leaderless MSS, the attitude stabilization and convergence to the desired attitude cannot be guaranteed, as observed in Fig. 5 (a), and Fig. 5(b). In addition, because the initial unit-quaternions $\boldsymbol{Q}_i(0)$ of the Spacecrafts $1, 3, 4$ and 6 are changed to $-\boldsymbol{Q}_i(0)$, the actual attitude of the spacecraft is not changed. However, the attitude stabilization errors of the two approaches are not equal, indicating that although the final attitude of the MSS has achieved attitude consensus, the converged attitude is different. This may lead to the failure of the observation mission. The process of angular velocity (Fig. 5(b) and Fig. 5)) and control torque (Fig. 5)) and Fig. 5(d)) also show that the attitude convergence of MSS based on unit-quaternion is different in Situation 2 and Situation 3. On the contrary, because the rotation represented by Lie group SO(3) is unique, the proposed controller Eq. (47) using SO(3)-based modeling method avoids this unwinding issue.

6.2. Comparison of different stochastic links failure modelings

In the previous subsection, the connectivity of the communication links is considered to be nondeterministic at each sampling instance, i.e., the failure or reconstruction of the link connection may occur at each sampling instance (cf.

Uncorrected Proof

Please cite this article in press as: KANG Z et al. Attitude control of multi-spacecraft systems on SO(3) with stochastic links failure, *Chin J Aeronaut* (2023), https://doi.org/10.1016/j.cja.2023.12.019

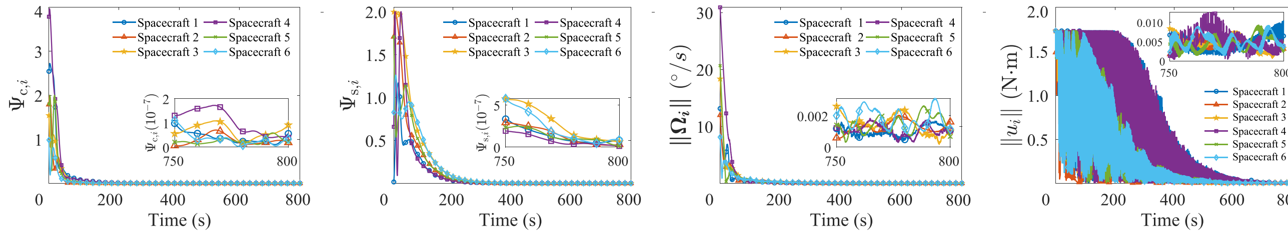

(a) Attitude consensus error (b) Attitude stabilization error (c) Angular velocity (d) Control torque

Fig. 3 Time history of attitude state of each spacecraft in MSS under Situation 1.

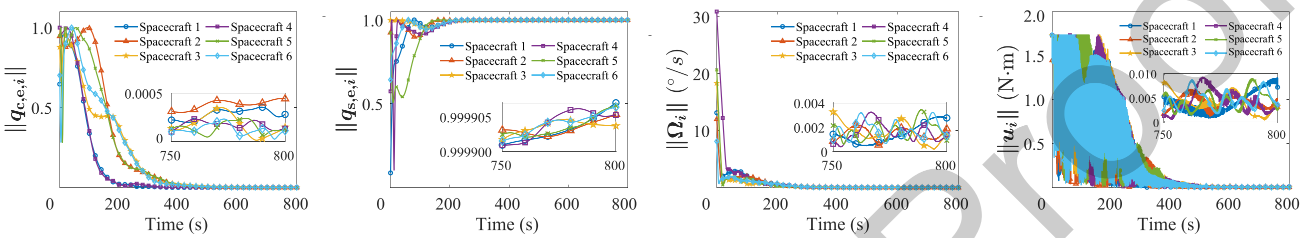

(a) Attitude consensus error (b) Attitude stabilization error (c) Angular velocity (d) Control torque

Fig. 4 Time history of attitude state of each spacecraft in MSS under Situation 2.

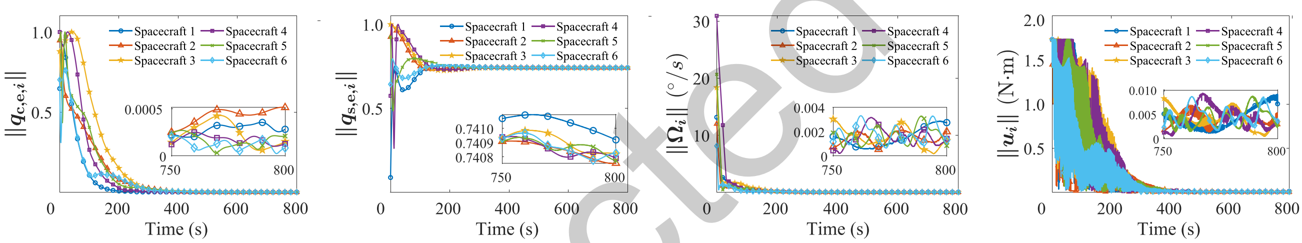

(a) Attitude consensus error (b) Attitude stabilization error (c) Angular velocity (d) Control torque

Fig. 5 Time history of attitude state of each spacecraft in MSS under Situation 3.

$T_{\text{step}} = 0.02$ s), which could result in too fast connectivity change. In practice, the connectivity of the link can be regarded as unchanged in every finite time interval T, i.e., the links failures happen in a periodic manner. We consider different methods of selecting the instance d_k, at which the stochastic communication failures occur, to model the periodically happened stochastic links failures. Specifically, we consider the following three cases that the instance d_k is selected.

Case 1. The stochastic failure of each link occurs asynchronously, which is modeled by

$$d_k = \mathrm{mod}(t + (k-1)\Delta t, T)\ k = 1, 2, \cdots, 10 \tag{75}$$

Case 2. The stochastic failure of each link occurs concurrently, which is modeled by

$$d_k = \mathrm{mod}(t, T)\ k = 1, 2, \cdots, 10 \tag{76}$$

Case 3. The stochastic links failure does not occur, i.e., the communication links are always connected. That is, $\forall t$, controller Eq. (47) with $a_{i,j}(p_{i,j}) = a_{i,0}(p_{i,0}) = 1$, where $i \in \{1, 2, \cdots, 6\}$ and $j \in \mathcal{N}_i$. where $\Delta t = 3$ s and $T = 27$ s denote the time delay and the generation interval in the simulation, respectively. In addition, $\mathrm{mod}(a, m)$ is the modulo operation and returns the remainder after division of a by m. Then, the value of d_k can be used to determine whether a new random number is generated for the l_k-th link. If $d_k = 0$, a new random number $c_{i,j}$ or $c_{i,0}$ is generated, otherwise the previous random number is maintained. These simulate the periodic occurrence of stochastic links failure.

In this subsection, the performance of the SO(3)-based leader–follower MSS using the proposed controller Eq. (47) under the foregoing three stochastic links failure modeling methods is compared. The controller parameters of Eq. (47) $k_1 = k_2 = 0.6, k_3 = 10$ are selected to satisfy condition Eq. (56).

Figs. 6–8 show the time history of attitude consensus error, attitude stabilization error, angular velocity and control torque of each spacecraft on SO(3) under the proposed controller Eq. (47) with three modeling methods of the stochastic links failure, respectively. It is observed that the proposed controller Eq. (47) can realize attitude consensus and attitude stabilization control of the MSS under different modeling methods of the stochastic links failure. When the stochastic links failure does not change at the same time (Case 1), the complexity of the control problem increases. On one hand, both the attitude consensus convergence speed and attitude stabilization convergence speed are slower than those when the stochastic links failure changes at the same time (Case 2), or those without stochastic links failure (Case 3). On the other hand, the conver-

Uncorrected Proof

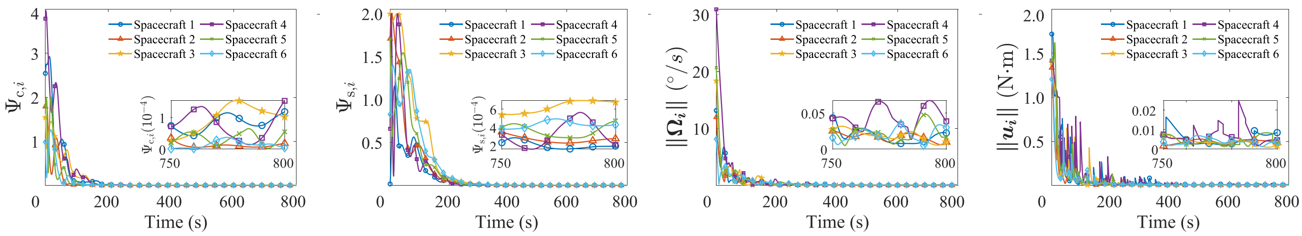

(a) Attitude consensus error (b) Attitude stabilization error (c) Angular velocity (d) Control torque

Fig. 6 Time history of attitude state of each spacecraft on SO(3) proposed controller Eq. (47), in which the stochastic links failure model is constructed as Case 1.

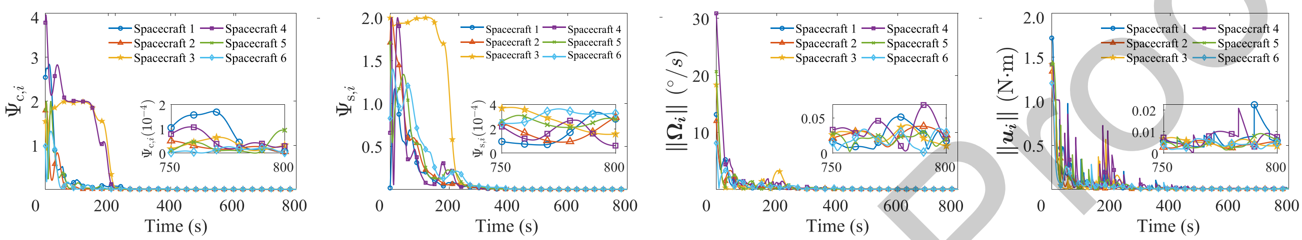

(a) Attitude consensus error (b) Attitude stabilization error (c) Angular velocity (d) Control torque

Fig. 7 Time history of attitude state of each spacecraft on SO(3) under proposed controller Eq. (47) in Case 2.

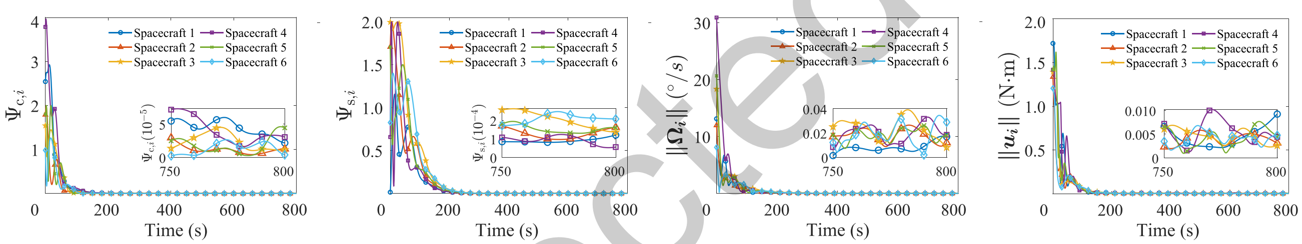

(a) Attitude consensus error (b) Attitude stabilization error (c) Angular velocity (d) Control torque

Fig. 8 Time history of attitude state of each spacecraft on SO(3) under proposed controller Eq. (47) in Case 3.

Table 2 Comparison of three stochastic links failure modeling methods.

Case No.	Consensus Steady-state $\Psi_{c,i}$		Stabilization Steady-state $\Psi_{s,i}$		Angular velocity Steady-state $\|\boldsymbol{\Omega}_i\|$ (°/s)	
	500 s	750 s	500 s	750 s	500 s	750 s
Case1	2.8×10^{-5}	8×10^{-7}	1.8×10^{-4}	3×10^{-6}	0.025	5×10^{-3}
Case2	1.2×10^{-5}	1.5×10^{-7}	8.5×10^{-4}	4×10^{-7}	0.02	2×10^{-3}
Case3	1.6×10^{-6}	2.3×10^{-9}	1×10^{-5}	2×10^{-8}	3.5×10^{-3}	1.5×10^{-4}

gence accuracy is lower than that of the other two stochastic links failure modeling methods, and more detailed comparison is shown in Table 2. It is considered that the stochastic links failure will delay the time of attitude convergence and cause the jump fluctuation of controller output.

In addition, it is noted that the stochastic links failure model of Situation 1 of the previous subsection is constructed to occur at each sampling time ($T_{\text{step}} = 0.02$ s), resulting in high-frequency oscillation of control torque (cf. Fig. 3(d)) due to the frequent link failures. This is an extreme situation in actual space missions, and may occur rarely. In real MSS, the stochastic links failure modes in Case 1 and Case 2 of this subsection may be more practical, and the high-frequency oscillation of the control torque in Fig. 3(d) can be avoided, as shown in Fig. 3(d) and Fig. 7(d).

7. Conclusions

In this paper, an attitude controller of the leader–follower multi-spacecraft system on SO(3) is proposed to realize attitude consensus and attitude stabilization under the stochastic links failure and actuator saturation. It is suitable for the

Uncorrected Proof

multi-spacecraft system in a directed topology link and with a static virtual leader.

The main conclusions are drawn as follows:

(1) The proposed multi-spacecraft system attitude error model is based on SO(3) and considers that the attitude error on SO(3) cannot be defined based on algebraic subtraction.
(2) Despite the stochastic connectivity of the communication links, the proposed controller can achieve attitude consensus and attitude stabilization at the same time by leveraging the super-martingale convergence theory.
(3) Simulation results demonstrate the efficiency of the proposed attitude controller. The results show that the proposed controller for the multi-spacecraft system on SO(3) can avoid the fuzziness of the unit-quaternion, and can realize attitude consensus and attitude stabilization control of the multi-spacecraft system under different modeling methods of stochastic links failure.

In future works, the attitude control of multi-spacecraft system under the stochastic failure of communication link and the change of communication topology will be explored.

Data availability

Declaration of Competing Interest

The authors declare that they have no known competing financial interests or personal relationships that could have appeared to influence the work reported in this paper.

Acknowledgements

This work was supported in part by the National Natural Science Foundation of China (Nos. U20B2054, U20B2056 and 62103275), and the Natural Science Foundation of Shanghai, China (No. 23ZR1 432400).

References

1. Gao H, Xia Y, Zhang J, et al. Finite-time fault-tolerant output feedback attitude control of spacecraft formation with guaranteed performance. *Int J Robust Nonlinear Control* 2021;**31**(10):4664–88.
2. Ren W, Beard RW. Decentralized scheme for spacecraft formation flying via the virtual structure approach. *J Guid, Control, Dynam* 2004;**27**(1):73–82.
3. Alfriend KT, Vadali SR, Gurfil P, et al. *Spacecraft formation flying: Dynamics, control and navigation*, Vol. 2. Amsterdam: Elsevier; 2009.
4. Lee D, Sanyal AK, Butcher EA. Asymptotic tracking control for spacecraft formation flying with decentralized collision avoidance. *J Guid, Control, Dynam* 2015;**38**(4):587–600.
5. Wei C, Luo J, Dai H, et al. Learning-based adaptive attitude control of spacecraft formation with guaranteed prescribed performance. *IEEE Trans Cybernet* 2018;**49**(11):4004–16.
6. Chaturvedi NA, Sanyal AK, McClamroch NH. Rigid-body attitude control. *IEEE Control Syst Mag* 2011;**31**(3):30–51.
7. Stuelpnagel J. On the parametrization of the three-dimensional rotation group. *SIAM Rev* 1964;**6**(4):422–30.
8. Guo Y, Song SM, Li XH. Finite-time output feedback attitude coordination control for formation flying spacecraft without unwinding. *Acta Astronaut* 2016;**122**:159–74.
9. Lee T. Global exponential attitude tracking controls on SO(3). *IEEE Trans Autom Control* 2015;**60**(10):2837–42.
10. Kulumani S, Poole C, Lee T. Geometric adaptive control of attitude dynamics on SO(3) with state inequality constraints*2016 American control conference (ACC)*. Piscataway: IEEE Press; 2016. p. 4936–41.
11. Chen T, Shan J, Wen H. Distributed adaptive attitude control for networked underactuated flexible spacecraft. *IEEE Trans Aerosp Electron Syst* 2018;**55**(1):215–25.
12. Liu Y, Huang P, Zhang F, et al. Distributed formation control using artificial potentials and neural network for constrained multiagent systems. *IEEE Trans Control Syst Technol* 2018;**28**(2):697–704.
13. Hu Q, Zhang J, Zhang Y. Velocity-free attitude coordinated tracking control for spacecraft formation flying. *ISA Trans* 2018;**73**:54–65.
14. Li J, Chen S, Li C, et al. Distributed game strategy for formation flying of multiple spacecraft with disturbance rejection. *IEEE Trans Aerosp Electron Syst* 2020;**57**(1):119–28.
15. Zhou Z, Zhang Z, Wang Y. Distributed coordinated attitude tracking control of a multi-spacecraft system with dynamic leader under communication delays. *Scient Rep* 2022;**12**(1):15048.
16. Du H, Chen MZ, Wen G. Leader–following attitude consensus for spacecraft formation with rigid and flexible spacecraft. *J Guid, Control, Dynam* 2016;**39**(4):944–51.
17. Cui B, Xia Y, Liu K, et al. Velocity-observer-based distributed finite-time attitude tracking control for multiple uncertain rigid spacecraft. *IEEE Trans Industr Inf* 2019;**16**(4):2509–19.
18. Zhang C, Wang J, Zhang D, et al. Fault-tolerant adaptive finite-time attitude synchronization and tracking control for multi-spacecraft formation. *Aerosp Sci Technol* 2018;**73**:197–209.
19. Yue X, Xue X, Wen H, et al. Adaptive control for attitude coordination of leader-following rigid spacecraft systems with inertia parameter uncertainties. *Chin J Aeronaut* 2019;**32**(3):688–700.
20. Hu Q, Li X, Wang C. Adaptive fault-tolerant attitude tracking control for spacecraft with time-varying inertia uncertainties. *Chin J Aeronaut* 2019;**32**(3):674–87.
21. Chen T, Shan J. Distributed spacecraft attitude tracking and synchronization under directed graphs. *Aerosp Sci Technol* 2021;**109**:106432.
22. Kang Z, Shen Q, Wu S, et al. Saturated attitude control of multi-spacecraft systems on SO(3) subject to mixed attitude constraints with arbitrary initial attitude. *IEEE Trans Aerosp Electron Syst* 2023;1–17.
23. Rezaee H, Parisini T, Polycarpou MM. Almost sure resilient consensus under stochastic interaction: Links failure and noisy channels. *IEEE Trans Autom Control* 2021;**66**(12):5727–41.
24. Rezaee H, Abdollahi F. Robust attitude alignment in multispacecraft systems with stochastic links failure. *Automatica* 2020;**118**:109033.
25. Lee T. Exponential stability of an attitude tracking control system on SO(3) for large-angle rotational maneuvers. *Syst Control Lett* 2012;**61**(1):231–7.
26. Lee T, Chang DE, Eun Y. Attitude control strategies overcoming the topological obstruction on SO(3)*2017 American control conference (ACC)*. Piscataway: IEEE Press; 2017. p. 2225–30.
27. Chen M, Shi P, Lim CC. Robust constrained control for MIMO nonlinear systems based on disturbance observer. *IEEE Trans Autom Control* 2015;**60**(12):3281–6.
28. Wang Q, Su CY. Robust adaptive control of a class of nonlinear systems including actuator hysteresis with Prandtl-Ishlinskii presentations. *Automatica* 2006;**42**(5):859–67.

Uncorrected Proof

29. Mousavi SH, Khayatian A. Dead-zone model based adaptive backstepping control for a class of uncertain saturated systems. *IFAC Proc Vol* 2011;**44**(1):14489–94.
30. Williams D. *Probability with martingales*. Cambridge: Cambridge University Press; 1991.
31. Mahmoud M, Jiang J, Zhang Y. *Active fault tolerant control systems: Stochastic analysis and synthesis*, Vol. 287. Berlin, Heidelberg: Springer Science and Business Media; 2003.
32. Bauer H. *Probability theory*. Berlin: Walter de Gruyter; 1996.
33. Lewis FL, Zhang H, Hengster-Movric K, et al. *Cooperative control of multi-agent systems: Optimal and adaptive design approaches*. Heidelberg: Springer Science and Business Media; 2013.
34. Kulumani S, Lee T. Constrained geometric attitude control on SO (3). *Int J Control Autom Syst* 2017;**15**(6):2796–809.
35. Barkana I. Defending the beauty of the invariance principle. *Int J Control* 2014;**87**(1):186–206.
36. Lee U, Mesbahi M. Feedback control for spacecraft reorientation under attitude constraints via convex potentials. *IEEE Trans Aerosp Electron Syst* 2014;**50**(4):2578–92.

Uncorrected Proof

Please cite this article in press as: KANG Z et al. Attitude control of multi-spacecraft systems on SO(3) with stochastic links failure, *Chin J Aeronaut* (2023), https://doi.org/10.1016/j.cja.2023.12.019